Integrated UAV Trajectory Control and Resource Allocation for UAV-Based Wireless Networks With Co-Channel Interference Management

Minh Dat Nguyen, *Graduate Student Member, IEEE*, Long Bao Le, *Senior Member, IEEE*, and André Girard, *Member, IEEE*

***Abstract*—In this article, we study the trajectory control, subchannel assignment, and user association design for unmanned aerial vehicles (UAVs)-based wireless networks. We propose a method to optimize the max-min average rate subject to data demand constraints of ground users (GUs) where spectrum reuse and co-channel interference management are considered. The mathematical model is a mixed-integer nonlinear optimization problem which we solve by using the alternating optimization approach where we iteratively optimize the user association, subchannel assignment, and UAV trajectory control until convergence. For the subchannel assignment subproblem, we propose an iterative subchannel assignment (ISA) algorithm to obtain an efficient solution. Moreover, the successive convex approximation (SCA) is used to convexify and solve the nonconvex UAV trajectory control subproblem. Via extensive numerical studies, we illustrate the effectiveness of our proposed design considering different UAV flight periods and number of subchannels and GUs as compared with a simple heuristic.**

***Index Terms*—Mixed-integer nonlinear programming, subchannel assignment, unmanned aerial vehicle (UAV) trajectory, user association.**

I. Introduction

NEXT-GENERATION wireless communications networks are expected to provide much higher capacity, lower latency, better communication reliability, and stability for billions of devices anywhere and anytime [1], [2]. However, deployment of an efficient fixed terrestrial wireless infrastructure can be quite challenging in certain scenarios, e.g., emergency situations, such as natural disasters and fast service recovery. To this end, unmanned aerial vehicle (UAV) communications can overcome certain limitations of a fixed wireless communications infrastructure where UAV communications can improve the coverage, users' Quality of Service (QoS), and the communication resilience and availability thanks to their attributes, such as mobility, flexibility, and controllable altitude [3]–[6].

The design of effective UAV-enabled communications networks, however, is quite challenging [3]. First, channel modeling for different UAV communication is a major research challenge. Specifically, communication channels for air-to-ground (A2G) communications between UAVs and ground users (GUs) must be appropriately modeled considering possible Line-of-Sight (LoS) and Non-Line-of-Sight (NLoS) propagation conditions. Second, efficient deployment of UAVs in 3-D space or effective control of UAVs' trajectories significantly impacts communications performance, such as UAV's flight time, energy consumption, and GUs' QoS. Finally, the development of resource allocation algorithms that can efficiently manage and assign various types of network resources, including communication bandwidth and transmit power for users, is of critical importance for UAV-enabled communications networks.

Generally, UAVs can act as mobile users, relays, or flying base stations (BSs) to enhance the coverage and capacity of wireless networks. There has been a great deal of research on these UAV communications scenarios in recent years. In particular, research on data collection for wireless nodes in wireless sensor networks (WSNs) and Internet of Things (IoT) leveraging the UAV communication has been an active research topic [7]–[10]. In [7], a cellular-enabled UAV communication setting with given UAV's initial and final locations of a single UAV was considered where the design goal was to minimize the UAV's mission completion time by optimizing its trajectory. The optimization of the UAV's trajectory was also studied in [8] for a WSN where one UAV is used as a mobile data collector to minimize the maximum energy consumption of all sensor nodes. Similarly, Ghorbel *et al.* [9] proposed an energy-efficient framework for a WSN using a flying UAV whose stopping positions were optimized for efficient data collection. Finally, placement optimization for multiple UAVs was studied to achieve low overhead and high sensor search accuracy in [10].

There has also been much work for UAV-enabled wireless networks in which UAVs act as relays [11]–[15]. Specifically, 2-D placement or trajectory optimization of UAVs have been studied where UAVs are mostly assumed to stay at a fixed altitude. The joint power and UAV's trajectory optimization to maximize the end-to-end throughput from a source to its destination for the UAV-based relay network was also studied in [11], For the network setting with multiple UAVs, Fan *et al.* [12] considered the joint optimization of the power, bandwidth allocation, and UAVs' trajectories to maximize the

Manuscript received November 2, 2021; accepted December 20, 2021. Date of publication December 24, 2021; date of current version July 7, 2022. *(Corresponding author: Minh Dat Nguyen.)*

The authors are with the Institut National de la Recherche Scientifique—Énergie, Matériaux et Télécommunications, University of Québec, Montréal, QC H5A 1K6, Canada (e-mail: minh.dat.nguyen@inrs.ca; long.le@inrs.ca; andre@inrs.ca).

Digital Object Identifier 10.1109/JIOT.2021.3138374

average end-to-end throughput. Wang *et al.* [13] studied a UAV-to-ground secure communication system with a single UAV relay at a fixed altitude and multiple eavesdroppers. Here, the design objective is to maximize the minimum secrecy rate by jointly optimizing the transmit power and location of the UAV. Moreover, by using a UAV full-duplex relay at a fixed altitude, Wang *et al.* [14] jointly optimized the transmit power and UAV's trajectory to achieve the maximum destination node's throughput considering spectrum sharing with terrestrial device-to-device (D2D) communications. Fan *et al.* [15] considered the 3-D placement of a single UAV acting as a relay for a network with multiple communication pairs of source and destination nodes on the ground. Here, the design objective was to maximize the network throughput by jointly optimizing the transmit power, bandwidth allocation, and UAV placement.

Finally, UAVs can serve as aerial BSs to provide on-the-fly communications and enhance the performance of the terrestrial wireless networks. In fact, UAV placement and trajectory control optimization have been studied in [16]–[22]. For the UAV placement, Al-Hourani *et al.* [16] proposed an analytical framework to optimize the UAV's altitude providing maximum coverage. Lyu *et al.* [17] optimized the required number of UAVs and their positions to provide the best wireless coverage for a group of GUs. The joint bandwidth and power allocation for multihop UAV-based downlink communications was studied in [18] where orthogonal bandwidth allocation for both access and backhaul links was considered. In our previous work [19], we considered the joint placement for stationary UAVs and nonorthogonal bandwidth allocation for wireless access links. In [20], the joint optimization of power allocation and trajectory control for the frequency-division multiple access (FDMA) UAV-based wireless network was studied. In [21], the joint optimization of user association, power allocation, and UAV's trajectory control for the wireless network with multiple UAVs was considered assuming no co-channel interference. Moreover, Wu *et al.* [22] jointly optimized the scheduling, user association, power allocation, and UAV's trajectory control for the time-division multiple access (TDMA)-based wireless network.

While the papers mentioned above have considered the optimization of the UAV placement or UAV trajectory control and resource allocation in different network settings, there are still various research issues deserving more in-depth studies. In particular, spectrum reuse to support communications between multiple UAVs and GUs is needed in practice to enhance the spectrum efficiency and network performance; however, efficient co-channel interference management techniques must be developed. Moreover, many practical application scenarios, such as data collection, information sharing require to guarantee data transmission demand constraints of individual GUs. To fill these research gaps, we study in this article the joint UAV-GU association, resource allocation, and UAV trajectory control for UAV-based wireless networks with spectrum reuse and interference management. The main contributions can be summarized as follows.

1) We formulate the joint UAV-GU association, UAV trajectory control, and nonorthogonal subchannel assignment problem for UAV-based wireless networks. We maximize the minimum average rate of all GUs considering constraints on data transmission demands of individual GUs.
2) We solve the underlying mixed-integer nonlinear optimization problem (MINLP) problem using the alternating optimization approach. We solve the UAV-GU association, subchannel assignment, and UAV trajectory control subproblems separately in each iteration until convergence. We develop an iterative subchannel assignment (ISA) algorithm to tackle the subchannel assignment subproblem. Given the UAV-GU association and subchannel assignment solutions, the UAV trajectory control subproblem is a difficult nonconvex problem. We propose to use the successive convex approximation (SCA) technique to convexify and solve this subproblem. We then present a short complexity analysis of the proposed algorithm.
3) Extensive numerical results are presented to show the performance of our algorithm. Specifically, we compare the network performance when the proposed ISA subchannel algorithm and a baseline heuristic subchannel assignment with the interference management (SAIM) algorithm are used to solve the joint problem. We also study the impacts of different parameters and the importance of trajectory control on the achievable performance. Finally, we illustrate the convergence of the algorithm.

The remainder of this article is organized as follows. In Section II, we discuss the related work on joint optimization of UAV trajectory control and bandwidth allocation. Section III presents the system model and problem formulation. In Section IV, we describe how we solve the three subproblems and provide the convergence and complexity analysis of the proposed algorithm. Section V presents the numerical results for performance evaluations of the algorithm. Finally, Section VI concludes this work.

II. Related Work

A summary of recent work on joint UAV trajectory control and bandwidth allocation is given in Table I. In fact, data transmission demand constraints and spectrum reuse with interference management have a significant impact on the achievable performance of UAV-based wireless networks; however, taking the these aspects into account makes the design very challenging. Therefore, we include these design aspects in addition to others for related works in Table I. This table confirms that our current work considers all key design aspects and provides fairness for GUs by maximizing the minimum average rate of the GUs so that our work presents a more extensive design framework for UAV-based wireless networks compared to the existing literature.

On the one hand, this article [23] jointly optimized the power, continuous bandwidth assignment, and 3-D UAV's trajectory where the objective is to minimize the total UAV's energy consumption. This work did not consider data transmission demand constraints and co-channel interference. A block coordinate descent algorithm was used to iteratively

TABLE I
RELATED WORK ON UAV TRAJECTORY AND BANDWIDTH ALLOCATION FOR UAV-BASED WIRELESS NETWORKS

Ref.	Type	Objective	Data Demand Constraint	Trajectory Optimization	Bandwidth Allocation	Spectrum Reuse
[23]	Single UAV	Minimize UAV energy consumption	No	Yes	Continuous bandwidth assignment	No
[24]	Single UAV	Maximize system energy efficiency	Yes	Yes	Continuous bandwidth assignment	No
[25]	Single UAV	Maximize minimum average rate of delay-tolerant users	Yes	Yes	Continuous bandwidth assignment	No
[26]	Multiple UAVs	Maximize uplink sum-rate	Yes	No	Sub-channel assignment	Yes
[27]	Multiple UAVs	Maximize system energy efficiency	Yes	Yes	Sub-channel assignment	Yes
[28]	Single UAV	Maximize minimum average rate of GUs	No	Yes	Sub-channel assignment	No
[29]	Single UAV	Maximize minimum average rate of GUs	Yes	Yes	Sub-channel assignment	No
[30]	Multiple UAVs	Maximize minimum average rate of GUs	Yes	Yes	Sub-channel assignment	Yes
This Work	Multiple UAVs	Maximize minimum average rate of GUs	Yes	Yes	Sub-channel assignment	Yes

optimize the resource allocation and UAV's trajectory control. Zeng *et al.* [24] addressed the joint design of user scheduling, transmit power, continuous bandwidth assignment, and UAV's trajectory control in the 3-D space to maximize the system energy efficiency. However, this work did not consider co-channel interference and an iterative algorithm using the Dinkelbach and block coordinate descent techniques was proposed to solve the problem. Huang *et al.* [25] also studied the UAV's trajectory and continuous bandwidth assignment without considering co-channel interference. The design goal was to maximize the minimum average rate of GUs using an alternating optimization technique.

On the other hand, the work [26]–[30] mainly studied the subchannel assignment and UAV trajectory control. An exception is [26] where the authors discussed the subchannel assignment while considering co-channel interference and UAV velocity control with a known trajectory to maximize the uplink sum rate through an iterative algorithm. Cai *et al.* [27] studied the network setting with only two UAVs, i.e., transmitter and jammer, to maximize the system energy efficiency by jointly optimizing the transmit power, subchannel assignment, and UAV trajectory control using an alternating optimization algorithm with a relaxation of the binary subchannel assignment decision variables. Moreover, the design in [28]–[30] was to maximize the minimum average rate of GUs. The co-channel interference was considered only in [30]. The subchannel assignment was investigated in [28] for a network where the UAV used orthogonal FDMA (OFDMA). Bandwidth, power allocation, and UAV's trajectory control were jointly optimized using the block coordinate descent method. A backhaul-aware design to maximize the minimum average rate for GUs was proposed in [29] and [30] using an alternating optimization approach to solve the joint problem of subchannel assignment and UAV's trajectory control.

Even though there has been some limited work on the joint subchannel assignment and UAV's trajectory design considering spectrum reuse and co-channel interference management, this research direction remains under-explored in the UAV communication literature. In our preliminary work [30], we developed a heuristic algorithm for the UAV trajectory control and subchannel assignment problem. The present work makes several significant extensions of this conference work. Specifically, we solve three subproblems, namely, the UAV-GU association, subchannel assignment, and UAV trajectory control, and develop an integrated algorithm to solve the joint optimization problem of UAV-GU association, subchannel assignment, and UAV trajectory control. Moreover, we give a complexity analysis and prove the convergence of the integrated algorithm. Finally, much more extensive numerical results are presented in this article compared to those in the conference paper to demonstrate the efficiency and desirable performance of the proposed algorithm.

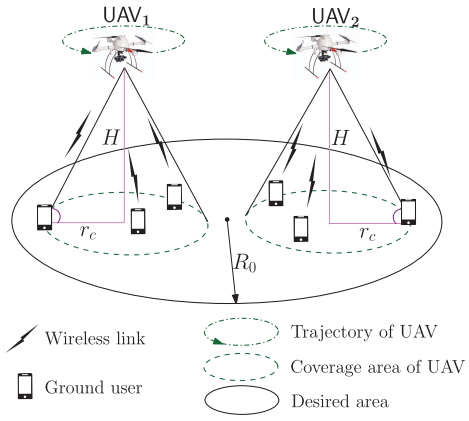

Fig. 1. UAV-based wireless network.

III. SYSTEM MODEL

We consider a network where a set of UAVs denoted as $\mathcal{M} = \{1, \ldots, M\}$, provides wireless connectivity for a set of GUs, denoted as $\mathcal{K} = \{1, \ldots, K\}$ as shown in Fig. 1.

We assume that each GU needs to receive a specific amount of data from UAVs in the downlink direction. This can be the case in many practical scenarios, e.g., GUs want to receive video files from the UAV such as specific scenes of a football match.

Because the UAVs are flying at a relatively high altitude, we assume that all communications, be it UAV-to-BS or UAV-to-GU, are dominated by LoS propagation.

The UAVs are assumed to be connected to the core network wirelessly through one cellular BS where the UAV-BS links are assumed to have sufficiently large capacity, i.e., by using mmWave communications. The assumption of LoS propagation for these channels is necessary because mmWave communications are very sensitive to blockage, which degrades the communication rate and reliability significantly. Also, the large bandwidth available at mmWave bands enables us to achieve the high capacity required by the backhaul links [31].

The UAV-GU channels, on the other hand, do not use mmWave communications since there are still many unresolved issues on the design of the hardware and physical layer for the transceivers deployed on UAV-based mmWave communications. For instance, more work is needed on highly directional antennas with efficient beamforming training and tracking to take into account the UAV movement and the channel Doppler effect. This is particularly difficult since the UAV's position and GUs discovery are tightly coupled [3]. For these reasons, we assume that only omni-directional antennas are installed on the UAVs to enable the low-complexity transceivers needed to achieve omnipresent coverage and dynamic GUs connections.

We assume that the UAVs fly at a fixed altitude H over a flight period of $T > 0$ seconds. The flight period is divided into N time slots where the set of time slots is denoted as $\mathcal{N} = \{1, \ldots, N\}$. At any time slot during the flight period T, each UAV can communicate with multiple GUs at the same time using OFDMA. The GUs are assumed to be located on the ground at zero altitude with fixed horizontal coordinates $\mathbf{r}_k^{\mathsf{u}} = (x_k^{\mathsf{u}}, y_k^{\mathsf{u}})\ \forall k \in \mathcal{K}$.

Let C be the number of subchannels available to support the wireless access links between UAVs and GUs. We denote the total transmit power of each UAV as $P_{\max} \geq 0$. We assume that the uniform power allocation is used by each UAV, i.e., the transmit power on each subchannel is equal the total transmit power $P_{\max}$ divided by the total subchannels used for downlink communications and is given by

$$p = \frac{P_{\max}}{C}. \tag{1}$$

The list of key notations in this article is given in Table II.

TABLE II
KEY NOTATIONS

Known Parameters	
C	Number of sub-channels
$\mathcal{C}$	Set of sub-channels
d_{min}	Minimum inter-UAV distance
D_k^{min}	Minimum data transmission demand of GU k
H	Fixed altitude of UAVs
K	Number of ground users (GUs)
$\mathcal{K}$	Set of GUs
M	Number of UAVs
$\mathcal{M}$	Set of UAVs
N	Total time slots
$P_{\max}$	Total transmit power of UAV
p	Transmit power on each sub-channel $(p = P_{\max}/C)$
$\mathbf{r}_k^{\mathsf{u}}$	Fixed horizontal coordinate of GU k $\left(\mathbf{r}_k^{\mathsf{u}} = (x_k^{\mathsf{u}}, y_k^{\mathsf{u}})\right)$
r_0	Center location of the considered network area
R_0	Radius of the considered network area
r_{c}	Radius of the circular cluster area
σ^2	Power of the additive white Gaussian noise (AWGN)
T	Flight period
Δt	Element slot length $(\Delta t = T/N)$
$V_{\max}$	Maximum speed of UAV
S_{max}	Maximum horizontal distance that the UAV can travel in each time slot $\left(S_{\mathsf{max}} \triangleq V_{\max}\Delta t\right)$
W	Bandwidth of each sub-channel
Decision and Auxiliary Variables	
$\omega_{k,m}[n]$	Association between UAV m and GU k in time slot n
$\theta_{z,c}[n]$	The sub-channel c is assigned to GU k in time slot n
$\mathbf{q}_m[n]$	Time-variant horizontal coordinate of the UAV m in time slot n $\left(\mathbf{q}_m[n] = (x_m^{\mathsf{d}}[n], y_m^{\mathsf{d}}[n])\right)$
$\mathbf{\Omega}$	Vector of all UAVs-GUs association decision variables $\mathbf{\Omega} = \{\omega_{k,m}[n], \forall k, m, n\}$
$\mathbf{\Theta}$	Vector of all sub-channel assignment decision variables $\mathbf{\Theta} = \{\theta_{k,c}[n], \forall k, c, n\}$
$\mathbf{Q}$	Vector of all time-variant horizontal coordinate of the UAVs $\mathbf{Q} = \{\mathbf{q}_m[n], \forall m, n\}$
η	Minimum average rate of all GUs $\left(\eta\left(\mathbf{\Omega}, \mathbf{\Theta}, \mathbf{Q}\right) = \min_{k\in\mathcal{K}} \bar{R}_k\right)$
Functions	
$\mathcal{C}_m[n]$	Set of sub-channels used by UAV m in time slot n $\lvert\mathcal{C}_m[n]\rvert = \sum_{k=1}^{K}\sum_{c=1}^{C}\omega_{k,m}[n]\theta_{k,c}[n]$, where $\lvert\mathcal{C}_m[n]\rvert$ denotes the number of sub-channels used by UAV m in time slot n
$d_{k,m}[n]$	Distance between UAV m and GU k in time slot n
$g_{k,m}[n]$	Channel power gain from UAV m and GU k in time slot n
$\gamma_{k,m,c}[n]$	Signal-to-interference-plus-noise ratio (SINR) at GU k served by UAV m in time slot n
ρ_0	Channel power gain at the distance of 1 m
$R_{k,m,c}[n]$	Achievable rate of GU k served by UAV m in time slot n on the sub-channel c
$R_k[n]$	Total rate achieved by GU k in time slot n
$\bar{R}_k$	Average rate per all slots of GU k

A. UAV-GU Association

Given the locations of the UAVs in each time slot, GUs need to be associated with the UAVs offering high-quality communications. For this, we define the binary UAV-GU association decision variable $\omega_{k,m}[n]$ which is equal to 1 if GU k is served by UAV m in time slot n and equal to 0, otherwise. Since each GU is associated with exactly one UAV in each time slot, they must meet the constraints

$$\sum_{m=1}^{M} \omega_{k,m}[n] = 1\ \forall k, n. \tag{2}$$

B. Subchannel Assignment

In addition to the UAV assignment, let W (MHz) denote the bandwidth of each subchannel and $\mathcal{C} = \{1, \ldots, C\}$ denote the set of subchannels. Besides, we have to decide the set of subchannels to be assigned for each GU. The corresponding decision variables are defined as

$$\theta_{k,c}[n] = \begin{cases} 1, \text{ if sub-channel } c \text{ is assigned to GU } k \\ \quad \text{in time slot } n \\ 0, \text{ otherwise.} \end{cases}$$

The first requirement for the assignment is that each GU must be assigned at least one subchannel at all times in order to maintain a continuous communication. This can be

expressed as

$$\sum_{c=1}^{C} \theta_{k,c}[n] \geq 1 \ \forall k, n. \tag{3}$$

Another constraint on the assignment is that for a given UAV, a subchannel can be used to support only one GU. This leads to a coupling between the ω and θ variables expressed as

$$\sum_{k=1}^{K} \omega_{k,m}[n]\theta_{k,c}[n] \leq 1 \ \forall m, n, c. \tag{4}$$

This constraint is the reason why we need to distinguish between the channels, even though they all have the same bandwidth.

C. UAV Trajectory Control

We optimize the UAVs' trajectories over the flight period T. This can be typically performed to achieve performance targets in data throughput and delay [22]. We assume that the UAV's energy is sufficiently large to cover its flight operation and wireless communications over the flight period T. This assumption is supported by [32] where a UAV equipped with a 3-cell, 3250 mAh, and 11.1-V LiPo battery can have a flight time of about 20 min.

The horizontal coordinate of UAV m in time slot n is denoted as $\mathbf{q}_m[n] = (x_m^{\mathsf{d}}[n], y_m^{\mathsf{d}}[n])$. We assume that each UAV m must come back to its initial position at the end of the flight period, i.e., its trajectory must satisfy the following constraint:

$$\mathbf{q}_m[1] = \mathbf{q}_m[N] \ \forall m \in \mathcal{M}. \tag{5}$$

The slot interval $\Delta t = T/N$ is set sufficiently small so that each UAV just flies a small distance during each time slot even at the maximum speed $V_{\max}$. Hence, the UAVs' trajectories must satisfy the following constraints:

$$\|\mathbf{q}_m[n+1] - \mathbf{q}_m[n]\|^2 \leq S_{\mathsf{max}}^2, n = 1, \ldots, N-1 \ \forall m \tag{6}$$

$$\left\|\mathbf{q}_m[n] - \mathbf{q}_j[n]\right\|^2 \geq d_{\mathsf{min}}^2 \ \forall n, m, j \neq m \tag{7}$$

where $\|.\|$ denotes the Euclidean norm, $S_{\mathsf{max}} \triangleq V_{\max}\Delta t$ is the maximum horizontal distance that the UAV can travel in each time slot, and d_{min} denotes the minimum inter-UAV distance and constraints (7) are imposed to ensure collision avoidance among UAVs.

D. Communication Model

Recall that we have assumed that the communication links from UAVs to GUs are dominated by the LoS propagation where the channel quality is mostly dependent on the UAV-GU distance. In time slot n, the distance between UAV m and GU k can be calculated as

$$d_{k,m}[n] = \sqrt{H^2 + \left\|\mathbf{q}_m[n] - \mathbf{r}_k^{\mathsf{u}}\right\|^2}. \tag{8}$$

The channel power gain from UAV m to GU k in time slot n on subchannel c is assumed to follow the free-space path loss model and it can be expressed as follows:

$$g_{k,m}[n] = \rho_0 d_{k,m}^{-2}[n] = \frac{\rho_0}{H^2 + \left\|\mathbf{q}_m[n] - \mathbf{r}_k^{\mathsf{u}}\right\|^2} \tag{9}$$

where ρ_0 presents the channel power gain at the reference distance of 1 m. The received signal to interference plus noise ratio (SINR) at GU k on subchannel c can be calculated as

$$\gamma_{k,m,c}[n] = \frac{pg_{k,m}[n]}{\sum_{j=1,j\neq m}^{M}\sum_{z=1,z\neq k}^{K}\omega_{z,j}[n]\theta_{z,c}[n]pg_{k,j}[n]+\sigma^2} \tag{10}$$

where σ^2 is the power of the additive white Gaussian noise (AWGN) at the receiver. The term $\sum_{j=1,j\neq m}^{M}\sum_{z=1,z\neq k}^{K}\omega_{z,j}[n]\theta_{z,c}[n]pg_{k,j}[n]$ represents the interference at GU k on the subchannel c due to the transmissions of other UAVs in time slot n on this subchannel. The achievable rate of GU k served by UAV m in time slot n on the subchannel c, denoted by $R_{k,m,c}[n]$ in bits/second (bps), can then be expressed as follows:

$$R_{k,m,c}[n] = \omega_{k,m}[n]\theta_{k,c}[n]W\log_2\big(1+\gamma_{k,m,c}[n]\big). \tag{11}$$

Therefore, the total rate achieved by GU k in time slot n, denoted by $R_k[n]$, can be written as

$$R_k[n] = \sum_{m=1}^{M}\sum_{c=1}^{C} R_{k,m,c}[n]. \tag{12}$$

As a result, the average rate per slot of GU k over N time slots can be expressed as follows:

$$\begin{aligned}\bar{R}_k &= \frac{1}{N}\sum_{n=1}^{N} R_k[n] \\ &= \frac{1}{N}\sum_{n=1}^{N}\sum_{m=1}^{M}\sum_{c=1}^{C}\omega_{k,m}[n]\theta_{k,c}[n]W\log_2\big(1+\gamma_{k,m,c}[n]\big).\end{aligned} \tag{13}$$

E. Problem Formulation

For convenience, we gather different decision variables as $\mathbf{\Omega} = \{\omega_{k,m}[n] \ \forall k, m, n\}$, $\mathbf{Q} = \{\mathbf{q}_m[n] \ \forall m, n\}$, and $\Theta = \{\theta_{k,c}[n] \ \forall k, c, n\}$. Our design goal is to maximize the minimum average rate achieved by all GUs by jointly optimizing the user association, i.e., $\mathbf{\Omega}$, subchannel assignment, i.e., Θ and UAV trajectory, i.e., $\mathbf{Q}$ over all time slots of the flight period.

The average rate $\bar{R}_k$ in (13) is a nonlinear function with respect to three decision variables $\mathbf{\Omega}, \Theta$, and $\mathbf{Q}$. Instead of performing the max-min optimization of this nonlinear function, we introduce the function $\eta(\mathbf{\Omega}, \Theta, \mathbf{Q}) = \min_{k\in\mathcal{K}} \bar{R}_k$ as the minimum average rate of all GUs. Then, our optimization problem becomes equivalent to maximizing $\eta(\mathbf{\Omega}, \Theta, \mathbf{Q})$, which is more tractable. Moreover, we assume that GU $k \ \forall k \in \mathcal{K}$, has the minimum data transmission demand of D_k^{min}, which must be received in the downlink direction over the UAV flight period. Then, the joint UAV-GU association, subchannel assignment, and UAV trajectory control optimization problem to maximize the minimum average rate over all GUs can be formulated as

$$\textbf{(P):} \max_{\eta,\boldsymbol{\Omega},\boldsymbol{\Theta},\mathbf{Q}} \quad \eta \tag{14}$$

$$\text{s.t.} \quad \bar{R}_k \geq \eta \ \forall k, \tag{14a}$$

$$\sum_{n=1}^{N} \Delta t R_k[n] \geq D_k^{\min} \ \forall k \tag{14b}$$

$$\|r_0 - \mathbf{q}_m[n]\| \leq R_0 \ \forall m, n \tag{14c}$$

$$\sum_{m=1}^{M} \omega_{k,m}[n] = 1 \ \forall k, n, \tag{14d}$$

$$\sum_{k=1}^{K} \omega_{k,m}[n]\theta_{k,c}[n] \leq 1 \quad \forall m, n, c \tag{14e}$$

$$\sum_{c=1}^{C} \theta_{k,c}[n] \geq 1 \quad \forall k, n \tag{14f}$$

$$\mathbf{q}_m[1] = \mathbf{q}_m[N] \quad \forall m \tag{14g}$$

$$\|\mathbf{q}_m[n+1] - \mathbf{q}_m[n]\|^2 \leq S_{\max}^2 \quad n = 1, \ldots, N-1 \tag{14h}$$

$$\left\|\mathbf{q}_m[n] - \mathbf{q}_j[n]\right\|^2 \geq d_{\min}^2 \ \forall n, m, j \neq m \tag{14i}$$

$$\omega_{k,m}[n] \in \{0, 1\} \quad \forall k, m, n \tag{14j}$$

$$\theta_{k,c}[n] \in \{0, 1\} \quad \forall k, c, n \tag{14k}$$

where R_0 represents the radius of the network area centered at r_0. Constraint (14b) captures the required data transmission demand for each GU over the flight period of T seconds. while constraints (14c) restrict the trajectories of all UAVs inside the desired network area. Moreover, (14d) and (14e) present the UAV-GU association constraints, (14e) and (14f) capture constraints on the subchannel assignment, and (14g)–(14i) represent constraints on the UAVs' trajectories. It can be seen that the constraints (14a), (14b), and (14i) are nonlinear and integer decision variables are involved in (14j) and (14k) for the UAV-GU association and subchannel assignment, respectively. Hence, problem (14) is an MINLP, which is difficult to solve optimally. In the following section, we describe how to compute good feasible solutions to this problem.

IV. Proposed Algorithm

We adopt the alternating optimization approach to solve problem (14) where we iteratively optimize each set of variables given the values of other variables in the corresponding subproblems until convergence. We describe how to solve these different subproblems in the following.

A. UAV-GU Association Given Subchannel Assignment and UAV Trajectory Control

For the given subchannel assignment $\boldsymbol{\Theta}$ and UAV trajectory $\mathbf{Q}$, the problem of optimizing the UAV-GU association $\boldsymbol{\Omega} = \{\omega_{k,m}[n] \ \forall k, m, n\}$ to achieve the max-min average rate over all GUs is still an integer nonlinear optimization problem. To make the problem more tractable, we relax the integer decision variables in $\boldsymbol{\Omega}$ into continuous decision variables, which yields the following problem:

$$\textbf{(P1.1)} : \max_{\eta,\boldsymbol{\Omega}} \quad \eta \tag{15}$$

$$\text{s.t.} \quad 0 \leq \omega_{k,m}[n] \leq 1 \ \forall k, m, n,$$
$$\text{constraints (14a), (14b), (14d), (14e).} \tag{15a}$$

Even with this relaxation, problem (15) is still a nonconvex optimization problem due to the nonconvex constraints (14a) and (14b). To this end, $R_{k,m,c}[n]$, in constraints (14a) and (14b), can be rewritten as follows:

$$R_{k,m,c}[n] = \omega_{k,m}[n]\theta_{k,c}[n]W \log_2\left(1 + \frac{p g_{k,m}[n]}{\sum_{j=1,j\neq m}^{M}\sum_{z=1,z\neq k}^{K} \omega_{z,j}[n]\theta_{z,c}[n] p g_{k,j}[n] + \sigma^2}\right) \geq \omega_{k,m}[n]\theta_{k,c}[n] W R_{k,m,c}^{\mathsf{A}}[n] \tag{16}$$

where

$$R_{k,m,c}^{\mathsf{A}}[n] \leq \log_2\left(1 + \frac{p g_{k,m}[n]}{\sum_{j=1,j\neq m}^{M}\sum_{z=1,z\neq k}^{K} \omega_{z,j}[n]\theta_{z,c}[n] p g_{k,j}[n] + \sigma^2}\right). \tag{17}$$

By introducing auxiliary variables $\mathbf{R}^{\mathsf{A}} = \{R_{k,m,c}^{\mathsf{A}}[n] \ \forall k, m, c, n\}$, problem (15) can be reformulated as

$$\textbf{(P1.1')} : \max_{\eta,\boldsymbol{\Omega},\mathbf{R}^{\mathsf{A}}} \quad \eta \tag{18}$$

$$\text{s.t.} \quad \frac{1}{N}\sum_{n=1}^{N}\sum_{m=1}^{M}\sum_{c=1}^{C} \omega_{k,m}[n] R_{k,m,c}^{\mathsf{A}}[n]\theta_{k,c}[n] W \geq \eta \tag{18a}$$

$$\sum_{n=1}^{N}\sum_{m=1}^{M}\sum_{c=1}^{C} \Delta t \omega_{k,m}[n] R_{k,m,c}^{\mathsf{A}}[n]\theta_{k,c}[n] W \geq D_k^{\min}$$
$$\text{constraints (14d), (14e), (15a), (17).} \tag{18b}$$

It can be seen that the constraints (17), (18a), and (18b) are still nonlinear. Thus, problem (18) is still a nonconvex optimization problem. To tackle this challenge, the successive convex optimization technique can be applied. First, let us consider the left-hand-side (LHS) of (18a) and (18b) with the variables of $\omega_{k,m}[n]$ and $R_{k,m,c}^{\mathsf{A}}[n]$, and based on the first-order Taylor expansion at the given points $\omega_{k,m}^{r}[n]$ and $R_{k,m,c}^{\mathsf{A},r}[n]$ in the rth iteration of the approximation process, we can obtain the following inequality:

$$\omega_{k,m}[n] R_{k,m,c}^{\mathsf{A}}[n] \geq \frac{1}{4}\Big[-\Big(\omega_{k,m}^{r}[n] + R_{k,m,c}^{\mathsf{A},r}[n]\Big)^2 + 2\Big(\omega_{k,m}^{r}[n] + R_{k,m,c}^{\mathsf{A},r}[n]\Big)\Big(\omega_{k,m}[n] + R_{k,m,c}^{\mathsf{A}}[n]\Big) - \Big(\omega_{k,m}[n] - R_{k,m,c}^{\mathsf{A}}[n]\Big)^2\Big] \triangleq R_{k,m,c}^{\mathsf{Alb},r}[n]. \tag{19}$$

Moreover, right-hand-side (RHS) of constraints (17) is convex with respect to $\omega_{z,j}[n]$. Thus, by applying the first-order Taylor expansion at the given points $\omega_{z,j}^{r}[n]$, we can obtain the lower bound $R_{k,m,c}^{\mathsf{AA},r}[n]$ as in (20), shown at the bottom of the next page.

Algorithm 1 SCA-Based Algorithm to Solve (18)

1: **Initialization:** Set $r := 0$, generate an initial point $\left(\mathbf{\Omega}^0, \mathbf{R}^{\mathsf{A},0}\right)$ of (21);
2: **repeat**
3: $r := r + 1$;
4: Solve (21) to obtain optimal values $\left(\mathbf{\Omega}^*, \mathbf{R}^{\mathsf{A},*}\right)$;
5: Update $\left(\mathbf{\Omega}^r, \mathbf{R}^{\mathsf{A},\mathsf{r}}\right) := \left(\mathbf{\Omega}^*, \mathbf{R}^{\mathsf{A},*}\right)$;
6: **until** Convergence
7: **Output** $\eta_{\mathsf{a}}^*, \mathbf{\Omega}^*, \mathbf{R}^{\mathsf{A},*}$.

Using the approximations above, problem (18) can be approximated by the following problem:

$$\textbf{(P1.1")}: \max_{\eta_{\mathsf{a}}^r, \mathbf{\Omega}, \mathbf{R}^{\mathsf{A}}} \quad \eta_{\mathsf{a}}^r \tag{21}$$

$$\text{s.t.} \quad \frac{1}{N}\sum_{n=1}^{N}\sum_{m=1}^{M}\sum_{c=1}^{C} R_{k,m,c}^{\mathsf{Alb},r}[n]\theta_{k,c}[n]W \geq \eta_{\mathsf{a}}^r \ \forall k \tag{21a}$$

$$\sum_{n=1}^{N}\sum_{m=1}^{M}\sum_{c=1}^{C} \Delta t R_{k,m,c}^{\mathsf{Alb},r}[n]\theta_{k,c}[n]W \geq D_k^{\min} \ \forall k \tag{21b}$$

$$R_{k,m,c}^{\mathsf{A}}[n] \leq R_{k,m,c}^{\mathsf{AA},r}[n] \ \forall k, m, c, n$$
$$\text{constraints (14d), (14e), (15a).} \tag{21c}$$

It can be seen that all constraints are linear. Hence, problem (21) is a standard convex optimization problem which can be solved efficiently by any convex optimization solvers such as CVX-Mosek [33]. A detailed description of our proposed algorithm to solve the UAV-GU association problem is given in Algorithm 1.

B. Subchannel Assignment Given UAV-GU Association and UAV Trajectory

For the given UAV-GU association and UAV trajectory $\{\mathbf{\Omega}, \mathbf{Q}\}$, we optimize the subchannel assignment $\mathbf{\Theta} = \{\theta_{k,c}[n] \ \forall k, c, n\}$ to achieve the max-min average rate among all GUs and this problem can be expressed as follows:

$$\textbf{(P2.1)}: \max_{\eta, \mathbf{\Theta}} \quad \eta$$
$$\text{s.t. constraints (14a), (14b), (14e), (14f), (14k).} \tag{22}$$

Proposition 1: Problem **(P2.1)** is NP-hard.

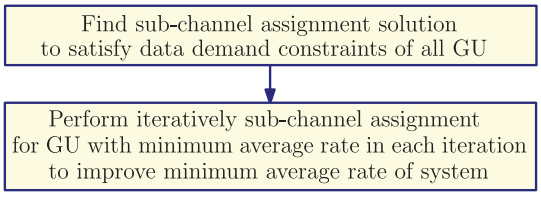

Fig. 2. Two main phases of proposed subchannel assignment algorithm.

Proof: The proof is given in Appendix A. ■

This integer nonconvex optimization problem is difficult to solve because subchannel assignments must be optimized over multiple UAVs, GUs, and time slots during the flight period. Hence, we propose a heuristic but efficient algorithm for subchannel assignments. Key phases of the proposed algorithm are described in Fig. 2.

Recall that our design objective is to maximize the minimum average rate among all GUs and satisfy the data transmission demands of individual GUs (i.e., $D_k^{\min}$ $\forall k \in \mathcal{K}$). Hence, in the first phase, we perform subchannel assignments for each GU to not only improve the design objective, but also ensure the constraints on data transmission demands of all GUs be satisfied. Specifically, we search a subchannel assignment for each GU k associated with UAV m in a certain time slot n to achieve a higher and maximum increase in the average rate of GU k and ensure the minimum average rate of the system not decreasing in each assignment step.

After the required data transmission demands of all GUs are satisfied, the algorithm enters an ISA loop where in each iteration, it searches the GU with the minimum average rate and finds the best subchannel assignment achieving the highest and better average rate for the underlying GU while improving the minimum average rate of the system. In fact, the method to determine the best subchannel assignment solution in this loop is similar to that in the previous phase. The algorithm terminates when the minimum average rate of all GUs cannot be improved further.

Details of the proposed algorithm called the *ISA Algorithm* are given in Algorithm 2. Let $D_k[n]$ denote the mount of data transmitted to GU k in time slot n. Then, the sum of $D_k[n]$ over different time slots of the flight period should be greater than the required data transmission demand for this GU, i.e., $D_k^{\min}$. In the first phase of the proposed algorithm, we perform subchannel assignments for each GU k until its required

$$\log_2\left(1+\frac{pg_{k,m}[n]}{\sum_{j\neq m}\sum_{z\neq k}\omega_{z,j}[n]\theta_{z,c}[n]pg_{k,j}[n]+\sigma^2}\right) \geq \log_2\left(1+\frac{pg_{k,m}[n]}{\sum_{j\neq m}\sum_{z\neq k}\omega_{z,j}^r[n]\theta_{z,c}[n]pg_{k,j}[n]+\sigma^2}\right) - \sum_{j\neq m}\sum_{z\neq k} A_{z,j,k,m,c}[n]\left(\omega_{z,j}[n]-\omega_{z,j}^r[n]\right) \triangleq R_{k,m,c}^{\mathsf{AA},r}[n] \tag{20}$$

where

$$A_{z,j,k,m,c}[n] = \frac{\omega_{z,j}^r[n]\theta_{z,c}[n]p^2 g_{k,j}[n]g_{k,m}[n]\log_2(e)}{\left(\sum_{j\neq m}\sum_{z\neq k}\omega_{z,j}^r[n]\theta_{z,c}[n]pg_{k,j}[n]+\sigma^2\right)\left(\sum_{j\neq m}\sum_{z\neq k}\omega_{z,j}^r[n]\theta_{z,c}[n]pg_{k,j}[n]+\sigma^2+pg_{k,m}[n]\right)}$$

Algorithm 2 ISA Algorithm

Require: M UAVs, K GUs, C sub-channels;
1: ***Given*:** UAV-GU association, UAV trajectory control;
Ensure: Max-min average rate ($\bar{R}_k$), η;
2: $k = 1$;
3: **while** $k \leq K$ **do**
4: **repeat**
5: Calculate the minimum average rate of the system: minrate $= \min_{k\in\mathcal{K}}\{\bar{R}_k\}$;
6: Given GU k, identify all UAV and time slot pairs $\{m, n\}$ with $\{\omega_{k,m}[n] = 1\}$;
7: Given GU k and each pair $\{m, n\}$ identified in step 6, find the sub-channel c for assignment to achieve the highest and better average rate for GU k;
8: Compare all potential sub-channel assignments for different pairs $\{m, n\}$ found in step 7, realize the best sub-channel assignment if it can improve the minimum average rate of the system (i.e., we calculate rate $= \min_{k\in\mathcal{K}}\{\bar{R}_k\}$ and the new sub-channel assignment must satisfy minrate $<$ rate);
9: **until** $\sum_n D_k[n] \geq D_k^{\min}$
10: $k \leftarrow k + 1$;
11: **end while**
12: **repeat**
13: Find GU $k = \text{argmin}_{k\in\mathcal{K}}\{\bar{R}_k\}$;
14: Calculate the minimum average rate of the system: minrate* $= \min_{k\in\mathcal{K}}\{\bar{R}_k\}$;
15: Given GU k, identify all UAV and time slot pairs $\{m, n\}$ with $\{\omega_{k,m}[n] = 1\}$;
16: Given GU k and each pair $\{m, n\}$ identified in step 15, find the sub-channel c for assignment to achieve the highest and better average rate for GU k;
17: Compare all potential sub-channel assignments for different pairs $\{m, n\}$ found in step 16, realize the best sub-channel assignment if it can improve the minimum average rate of the system (i.e., we calculate rate $= \min_{k\in\mathcal{K}}\{\bar{R}_k\}$ and the new sub-channel assignment must satisfy minrate* $<$ rate);
18: Update minrate* $=$ rate;
19: **until** Convergence
20: Update $\eta^* \leftarrow$ minrate*;
21: Return η^*, Θ^*.

data transmission demand is satisfied. Details of this phase are described from steps 4–9.

Specifically, the UAV serving a GU of interest is identified based on the UAV-GU association decision variable (i.e., $\omega_{k,m}[n] = 1$), which is the solution obtained from Section IV-A. In particular, step 6 identifies all potential pairs of UAV m and time slot n over the flight period for GU k. Then, we search the best subchannel c for one UAV and time slot pair (m, n) among those found in step 6 and perform the corresponding subchannel assignment, i.e., $\theta_{k,c}[n] = 1$, to achieve higher average rate for GU k while ensuring the minimum average rate of the system not decreasing. These steps are presented from steps 7 to 8. The subchannel assignment solution is identified by searching over all available subchannels and time slots for GU k while maintaining constraints (14e), (14f), and (14k). After performing the best subchannel assignment in a certain time slot for GU k, its data transmission demand constraint is verified. More subchannel assignments can be performed until the data transmission demand constraint of each GU k is satisfied.

Then, we attempt to improve the minimum average rate of the system in the following steps. In each subchannel assignment iteration, we find the GU k with the minimum average rate in step 13. For the identified GU k, we can find the best subchannel assignment in a certain time slot for this user and ensure the minimum average rate of the system not decreasing similar to that in the first phase. These steps are described from steps 14 to 17. After each subchannel assignment, the minimum average rate of the system is updated and the algorithm terminates when this value cannot be improved further.

C. UAV Trajectory Control Given UAV-GU Association and Subchannel Assignment

Given the UAV-GU association and subchannel assignment $\{\mathbf{\Omega}, \mathbf{\Theta}\}$, the problem optimizing the UAV trajectory control $\mathbf{Q} = \{\mathbf{q}_m[n]\ \forall m, n\}$ to achieve the max-min average rate over all GUs can be written as follows:

$$\textbf{(P3.1)}: \max_{\eta,\mathbf{Q}}\ \eta \quad \text{s.t. constraints (14a), (14b), (14c), (14g) (14h), (14i).} \tag{23}$$

This problem is a nonconvex optimization problem due to the nonconvex constraints (14a), (14b), and (14i). Therefore, it is difficult to solve this problem optimally. We design an algorithm with three main steps to solve this problem as follows. In step 1, we introduce some auxiliary variables and transform problem (23) into an equivalent form. Then, we approximately convexify the corresponding problem in step 2. Finally, we use a convex optimization solver to solve the obtained convex problem in step 3.

1) Step 1—Equivalent Transformation: We first rewrite the GU's achievable rate in the difference of convex functions (DC) form (more details can be found in Appendix B). First, we rewrite $R_{k,m,c}[n]$ in constraints (14a) as

$$R_{k,m,c}[n] = \omega_{k,m}[n]\theta_{k,c}[n]W\left(\hat{R}_{k,m,c}[n] - \tilde{R}_{k,m,c}[n]\right) \tag{24}$$

where

$$\hat{R}_{k,m,c}[n] = \log_2\left(\sum_{j=1}^{M}\sum_{z=1}^{K} R^{\mathsf{Ab}}_{z,j,c,k,m}[n] + \sigma^2\right) \tag{25}$$

$$\tilde{R}_{k,m,c}[n] = \log_2\left(\sum_{j=1,j\neq m}^{M}\sum_{z=1,z\neq k}^{K} R^{\mathsf{Ab}}_{z,j,c,k,m}[n] + \sigma^2\right) \tag{26}$$

in which

$$R^{\mathsf{Ab}}_{z,j,c,k,m}[n] = \frac{\omega_{z,j}[n]\theta_{z,c}[n]p\rho_0}{H^2 + \left\|\mathbf{q}_j[n] - \mathbf{r}_k^{\mathsf{u}}\right\|^2}. \tag{27}$$

We now introduce auxiliary variables $\mathbf{S} = \{S_{k,j}[n] \leq \left\|\mathbf{q}_j[n] - \mathbf{r}_k^{\mathsf{u}}\right\|^2\ \forall j, k, n\}$. Applying this to (27), we have

$$R^{\mathsf{Ab}}_{z,j,c,k,m}[n] \leq \frac{\omega_{z,j}[n]\theta_{z,c}[n]p\rho_0}{H^2 + S_{k,j}[n]}. \tag{28}$$

Then, problem (23) can be reformulated as

$$\textbf{(P3.1')}: \max_{\eta,\mathbf{Q},\mathbf{S},\mathbf{R}} \quad \eta \tag{29}$$

$$\text{s.t.} \quad \frac{1}{N}\sum_{n=1}^{N}\sum_{m=1}^{M}\sum_{c=1}^{C}\omega_{k,m}[n]\theta_{k,c}[n]W \left(\hat{R}_{k,m,c}[n]-\tilde{R}_{k,m,c}[n]\right)\geq \eta \ \forall k \tag{29a}$$

$$\sum_{n=1}^{N}\sum_{m=1}^{M}\sum_{c=1}^{C}\Delta t\omega_{k,m}[n]\theta_{k,c}[n]W \left(\hat{R}_{k,m,c}[n]-\tilde{R}_{k,m,c}[n]\right)\geq D_k^{\min} \ \forall k \tag{29b}$$

$$R^{\mathsf{Ab}}_{z,j,c,k,m}[n]\leq \frac{\omega_{z,j}[n]\theta_{z,c}[n]p\rho_0}{H^2+S_{k,j}[n]} \tag{29c}$$

$$S_{k,m}[n]\leq \left\|\mathbf{q}_m[n]-\mathbf{r}_k^{\mathsf{u}}\right\|^2 \ \forall k,m,n \tag{29d}$$

$$\|r_0-\mathbf{q}_m[n]\|\leq R_0 \ \forall m,n \tag{29e}$$

$$\mathbf{q}_m[1]=\mathbf{q}_m[N] \ \forall m \tag{29f}$$

$$\|\mathbf{q}_m[n+1]-\mathbf{q}_m[n]\|^2\leq S_{\max}^2,\ n=1,\ldots,N-1 \tag{29g}$$

$$\left\|\mathbf{q}_m[n]-\mathbf{q}_j[n]\right\|^2\geq d_{\min}^2 \ \forall n,m,j\neq m \tag{29h}$$

where $\mathbf{R}=\{R^{\mathsf{Ab}}_{z,j,c,k,m}[n],\forall k,m,z,j,c,n\}$.

It can be verified that $\hat{R}_{k,m,c}[n]$ and $\tilde{R}_{k,m,c}[n]$ are concave with respect to $R^{\mathsf{Ab}}_{z,j,c,k,m}[n]$. Moreover, constraints (29a) and (29b) are in the DC form. However, the constraints in (29c), (29d), and (29h) are still nonconvex so that problem (29) is still a nonconvex optimization problem.

2) Step 2—Convex Approximation: We can handle the nonconvex constraints (29a) and (29b) using the SCA technique. The nonconvex constraint functions are approximated by convex functions and the resulting optimization problem is solved iteratively. Specifically, we define $\mathbf{Q}^r=\{\mathbf{q}_m^r[n],\forall m,n\}$ to represent the trajectories of UAVs and $S_{k,j}^r[n]=\left\|\mathbf{q}_j^r[n]-\mathbf{r}_k^{\mathsf{u}}\right\|^2$ to denote the distance between UAVs and GUs in the rth iteration of this approximation. In addition, let $\mathbf{S}^r,\mathbf{R}^r$ be the achieved feasible variables in the rth iteration.

We now describe how to convexify this problem. We first consider $\tilde{R}_{k,m,c}[n]$ a concave function with respect to $R^{\mathsf{Ab}}_{z,j,c,k,m}[n]$. Recall that any concave function is upper-bounded by its first-order Taylor expansion at any point. Hence, we have

$$\tilde{R}_{k,m,c}[n]\leq \tilde{R}^{\mathsf{ub}}_{k,m,c}[n] \tag{30}$$

where $\tilde{R}^{\mathsf{ub}}_{k,m,c}[n]$ is described in more details in Appendix B.

In addition, constraints (29c) can be equivalently written as follows:

$$R^{\mathsf{Ab}}_{z,j,c,k,m}[n]S_{k,j}[n]\leq \omega_{z,j}[n]\theta_{z,c}[n]p\rho_0-R^{\mathsf{Ab}}_{z,j,c,k,m}[n]H^2.$$

We can express the LHS of this constraint in the DC form [34]. Hence, based on the first-order Taylor expansion at the given points $R^{\mathsf{Ab},r}_{z,j,c,k,m}[n]$ and $S_{k,j}^r[n]$ in the rth iteration of the approximation process, it can be approximated as

$$R^{\mathsf{Ab}}_{z,j,c,k,m}[n]S_{k,j}[n]\leq R^{\mathsf{App},r}[n] \tag{31}$$

where $R^{\mathsf{App},r}[n]$ is given in Appendix B. Thus, the constraints (29c) can be approximated as

$$\omega_{z,j}[n]\theta_{z,c}[n]p\rho_0-R^{\mathsf{Ab}}_{z,j,c,k,m}[n]H^2\geq R^{\mathsf{App},r}[n]. \tag{32}$$

Moreover, since $\left\|\mathbf{q}_m[n]-\mathbf{r}_k^{\mathsf{u}}\right\|^2$ in the constraints (29d) is a convex function with respect to $\mathbf{q}_m[n]$, we have the following inequality by applying the first-order Taylor expansion at the given point $\mathbf{q}_m^r[n]$:

$$\left\|\mathbf{q}_m[n]-\mathbf{r}_k^{\mathsf{u}}\right\|^2\geq \left\|\mathbf{q}_m^r[n]-\mathbf{r}_k^{\mathsf{u}}\right\|^2 + 2\left(\mathbf{q}_m^r[n]-\mathbf{r}_k^{\mathsf{u}}\right)^T\left(\mathbf{q}_m[n]-\mathbf{q}_m^r[n]\right). \tag{33}$$

Furthermore, by applying the first-order Taylor expansion at the given point $\mathbf{q}_m^r[n]$ and $\mathbf{q}_j^r[n]$ to $\left\|\mathbf{q}_m[n]-\mathbf{q}_j[n]\right\|^2$, the LHS of constraint (29h) can be approximated by its lower bound as

$$\left\|\mathbf{q}_m[n]-\mathbf{q}_j[n]\right\|^2\geq -\left\|\mathbf{q}_m^r[n]-\mathbf{q}_j^r[n]\right\|^2 + 2\left(\mathbf{q}_m^r[n]-\mathbf{q}_j^r[n]\right)^T\left(\mathbf{q}_m[n]-\mathbf{q}_j[n]\right) \ \forall j\neq m,n. \tag{34}$$

3) Step 3—Solving Approximated Convex Problem: Using the approximations above, problem (29) can be approximated as

$$\textbf{(P3.1'')}: \max_{\eta_{\mathsf{trj}}^r,\mathbf{Q},\mathbf{S},\mathbf{R}} \quad \eta_{\mathsf{trj}}^r \tag{35}$$

$$\text{s.t.} \quad \frac{1}{N}\sum_{n=1}^{N}\sum_{m=1}^{M}\sum_{c=1}^{C}\omega_{k,m}[n]\theta_{k,c}[n]W \left(\hat{R}_{k,m,c}[n]-\tilde{R}^{\mathsf{ub}}_{k,m,c}[n]\right)\geq \eta_{\mathsf{trj}}^r \ \forall k \tag{35a}$$

$$\sum_{n=1}^{N}\sum_{m=1}^{M}\sum_{c=1}^{C}\Delta t\omega_{k,m}[n]\theta_{k,c}[n]W \left(\hat{R}_{k,m,c}[n]-\tilde{R}^{\mathsf{ub}}_{k,m,c}[n]\right)\geq D_k^{\min} \ \forall k \tag{35b}$$

$$S_{k,m}[n]\leq \left\|\mathbf{q}_m^r[n]-\mathbf{r}_k^{\mathsf{u}}\right\|^2 + 2\left(\mathbf{q}_m^r[n]-\mathbf{r}_k^{\mathsf{u}}\right)^T\left(\mathbf{q}_m[n]-\mathbf{q}_m^r[n]\right) \ \forall k,m,n \tag{35c}$$

$$d_{\min}^2\leq -\left\|\mathbf{q}_m^r[n]-\mathbf{q}_j^r[n]\right\|^2 + 2\left(\mathbf{q}_m^r[n]-\mathbf{q}_j^r[n]\right)^T\left(\mathbf{q}_m[n]-\mathbf{q}_j[n]\right) \ \forall j\neq m,n$$

$$\text{(29e)–(29g), (32).} \tag{35d}$$

In this problem, constraints (29g) are convex while all remaining constraints are linear. Hence, problem (35) is a standard convex optimization problem which can be solved efficiently by any convex optimization solvers such as CVX-Mosek [33]. A detailed description of our proposed algorithm to solve the UAV trajectory control optimization problem is given in Algorithm 3.

Algorithm 3 SCA-Based Algorithm to Solve (23)

1: **Initialization:** Set $r := 0$, generate an initial point $\left(\mathbf{Q}^0, \mathbf{S}^0, \mathbf{R}^0\right)$ of (35);
2: **repeat**
3: $r := r + 1$;
4: Solve (35) to obtain optimal values $\left(\mathbf{Q}^*, \mathbf{S}^*, \mathbf{R}^*\right)$;
5: Update $\left(\mathbf{Q}^r, \mathbf{S}^r, \mathbf{R}^r\right) := \left(\mathbf{Q}^*, \mathbf{S}^*, \mathbf{R}^*\right)$;
6: **until** Convergence
7: **Output** $\eta^*_{\text{trj}}, \mathbf{Q}^*, \mathbf{S}^*, \mathbf{R}^*$.

Algorithm 4 Integrated UAV-GU Association, Subchannel Assignment, and UAV Trajectory Control

Require: M UAVs, K GUs, C sub-channels and T;
Ensure: Max-min average rate ($\bar{R}_k$), η; Let $r = 1$;
1: **repeat**
2: Optimize the UAV-GU association given the sub-channel assignment and UAVs' trajectories by solving sub-problem using Algorithm 1 to obtain $\mathbf{\Omega}^r$;
3: Optimize the sub-channel assignment given the UAV-GU association and UAVs' trajectories by solving sub-problem using Algorithm 2 to obtain Θ^r;
4: Optimize the UAVs' trajectories given the UAV-GU association and sub-channel assignment using Algorithm 3 to obtain $\mathbf{Q}^r$;
5: Update $r = r + 1$;
6: **until** Convergence
7: Return η^*, $\mathbf{\Omega}^*$, Θ^*, $\mathbf{Q}^*$.;

D. Integrated UAV-GU Association, Subchannel Assignment, and UAV Trajectory Control

Using the results presented in Sections IV-A–IV-C, our proposed algorithm based on the alternating optimization method is described in Algorithm 4. The convergence of this algorithm is stated in the following proposition.

Proposition 2: The proposed Algorithm 4 creates a sequence of feasible solutions where the objective value monotonically increases over iterations. As a result, the algorithm converges to a feasible solution.

Proof: The proof is given in Appendix C. ■

E. Complexity Analysis

We now analyze the complexity of our proposed algorithm evaluated in the number of required arithmetic operations. For the UAV-GU association subproblem, since CVX [33] invokes the interior-point method to solve the underlying problem (21), the involved complexity is $\mathcal{O}(m_1^{1/2}(m_1+m_2)m_2^2)$, where m_1 is the number of inequality constraints, m_2 denotes the number of variables [35], and $\mathcal{O}$ denotes the big-O notation. Hence, the complexity of this step is $\mathcal{O}(L_1 NK^{[7/2]})$, where L_1 is the number of iterations required to achieve the convergence of Algorithm 1.

We now analyze the complexity of the proposed ISA algorithm to solve the subchannel assignment subproblem, i.e., Algorithm 2. In the first phase of this algorithm, we find the subchannel assignment to satisfy the demand constraints for all GUs. For each GU, the required complexity is dominated by operations in steps 6–8, which investigate all sets of GUs, UAVs, subchannels, and time slots to identify the best assignment. The computational complexity is $\mathcal{O}(I_1(KMNC))$, where I_1 denotes the average number of iterations needed to ensure that the data transmission demand of each GU is satisfied. Hence, the complexity of this phase is $\mathcal{O}(I_1(K^2MNC))$. In the second phase, step 13 finds the UAV with the minimum average rate and its complexity is $\mathcal{O}(KMNC)$. In addition, steps 14–17 are similar to those in the first phase where the involved complexity is $\mathcal{O}(KMNC)$. Thus, the second loop has the computation complexity of $\mathcal{O}(2I_2(KMNC))$, where I_2 denotes the number of iterations needed to achieve convergence. Hence, the complexity of Algorithm 2 is $\mathcal{O}(I_1(K^2MNC) + 2I_2(KMNC))$.

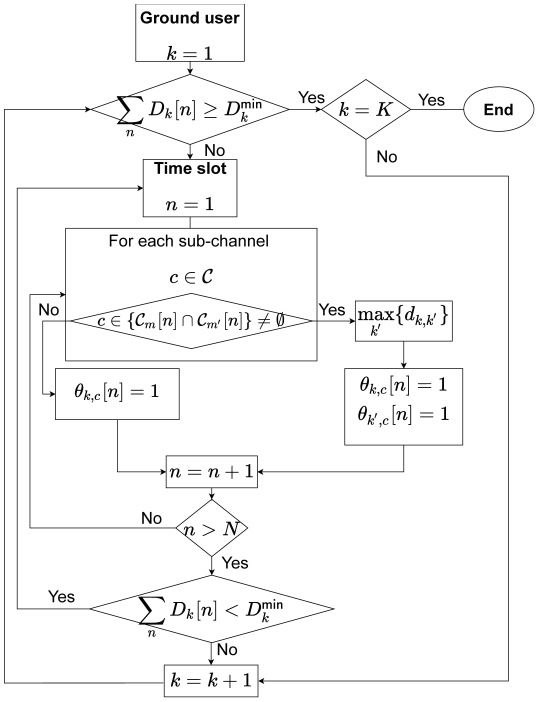

Fig. 3. SAIM.

We now analyze the complexity of the SCA-based Algorithm 3 to solve the UAV trajectory control subproblem. In step 4, we use the CVX solver to solve the convex optimization problem (35) by using the interior-point method with the complexity of $\mathcal{O}(L_2 NK^{7/2})$, where L_2 is the number of iterations required to achieve the convergence of Algorithm 3.

Let L denote the number of iterations needed in the outer loop to reach convergence for Algorithm 4. Then, the overall computation complexity of the proposed algorithm is $\mathcal{O}(L(I_1(K^2MNC) + 2I_2(KMNC)))$.

F. Heuristic Subchannel Assignment

For benchmarking purposes, an SAIM algorithm is presented whose key steps are illustrated in Fig. 3. The performance comparison between the SAIM and ISA algorithms are be discussed in Section V.

In the SAIM algorithm, we sequentially assign subchannels to each GU until its data transmission demand is satisfied. As a result, the constraint on the data transmission demand of each GU is tracked during the assignments to get a feasible

TABLE III
SIMULATION PARAMETERS

Parameter	Description	Value
M	Number of UAVs	$[2, 3]$
K	Number of GUs	$[8, 10, 12, 14, 16]$
C	Number of sub-channels	$[20, 30, 40, 50, 60]$
W	Bandwidth of each sub-channel	1 MHz
T	Flight period	$[20, 40]$ s
Δt	Length of each time slot	0.5 s
H	Altitude of UAVs	100 m
r_c	Radius of cluster	200 m
$P_{\max}$	Transmit power of UAV	30 dBm
σ^2	Noise power	-110 dBm
f_c	Carrier frequency	2.5 GHz
$d_{\min}$	Minimum inter-UAV distance	20 m
$V_{\max}$	Maximum speed of UAV	$[10 - 80]$ m/s

solution. The reason for this approach is to minimize utilizing a subchannel for different UAVs to mitigate the co-channel interference. In particular, the set of all subchannels, sets of subchannels used by UAVs m and m' in time slot n, which are denoted as $\mathcal{C}, \mathcal{C}_m[n]$, and $\mathcal{C}_{m'}[n]$, respectively, are investigated to perform each subchannel assignment. If all subchannels are assigned to GUs and certain data transmission demand constraints are still not satisfied, we reuse and allocate a subchannel already assigned for certain GU k' served by UAV $m' \neq m$ with maximum distance $d_{k,k'}$ from GU k of interest to mitigate the interference.

V. NUMERICAL RESULTS

A. Simulation Setting

In this section, we evaluate the performance of the proposed algorithm. The parameter setting for the simulations is similar to that in [22], [28], and [36] and are summarized in Table III. We consider a circular network area with radius $R_0 = 500$ m with two or more clusters, i.e., hotspots, of GUs. The radius of each circular cluster area is $r_{\mathsf{c}} = 200$ m and different clusters are placed far enough apart not to overlap. The distance between two neighboring clusters' centers is set to satisfy the following constraint $D^0 \geq d_{\min} + 2 \times r_{\mathsf{c}}(\mathrm{m})$. The altitude of all UAVs is assumed to be fixed at $H = 100$ m. Moreover, the required transmission data demand for each GU k ($D_k^{\min}$) is set according to the size of short videos, e.g., video files with the resolution of 30 frames per second (fps) [37]).

B. Algorithm Initialization

To execute our algorithm, we need to initialize the values of all variables. Here, we present a simple method to initialize the variables related to UAV-GU association and UAV trajectory control.

1) Initial UAV-GU Association: We assume that each GU k is initially associated with the UAV providing the highest average received signal strength (RSS) as follows:

$$\omega_{k,m}[n] = \begin{cases} 1, \ m = \arg\max\limits_{k} RSS_{k,m}[n] \\ 0, \ \text{otherwise} \end{cases} \tag{36}$$

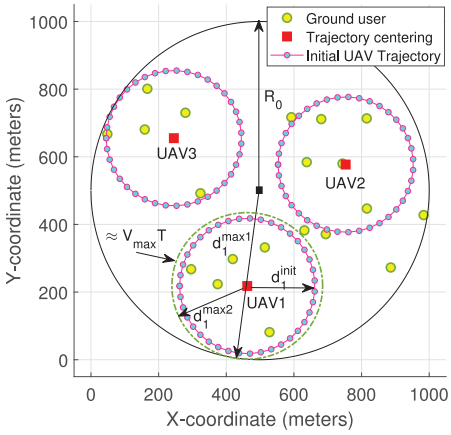

Fig. 4. Initial UAVs' trajectories.

where the average RSS for the GU k and UAV m can be expressed as

$$RSS_{k,m}[n](\mathrm{dBm}) = p(\mathrm{dBm}) - g_{k,m}[n](\mathrm{dBm}) \tag{37}$$

where p is the transmit power of UAV m used in its communication with GU k in time slot n on each assigned subchannel.

2) Initial Circular UAV Trajectory: To set the initial circular UAV trajectory, we assume that each UAV serves a circular network partition, i.e., serving a cluster of GUs, with radius r_{c} (m). For each network partition, we need to determine its center $\mathbf{c}_m^{\mathsf{init}} = (x_m^{\mathsf{init}}, y_m^{\mathsf{init}})$ and radius d_m^{init} for UAV m. These points are the centers of the corresponding network partitions computed using the k-means clustering algorithm [38] for given locations of the K GUs. The initial circular radius for UAV m is given by $d_m^{\mathsf{init}} = \min(d_m^{\mathsf{max1}}, d_m^{\mathsf{max2}}, r_{\mathsf{c}})$, where $d_m^{\mathsf{max1}} = R_0 - \left\| r_0 - \mathbf{c}_m^{\mathsf{init}} \right\|$ denotes the maximum radius of circular trajectory of UAV m. The UAV remains inside the desired area during the flight period and d_m^{max2} is the maximum radius of the circular UAV trajectory with the same starting and ending points.

To determine d_m^{max2}, we approximate the largest circumference of a circle as the maximum distance, denoted as $D = V_{\mathsf{max}} T$, that the UAV can travel during the flight period. Therefore, we have $d_m^{\mathsf{max2}} \approx D/2\pi$. Let $\phi_n \triangleq 2\pi[(n-1)/(N-1)]\ \forall n$, we can initialize $\mathbf{Q}^0 = \{\mathbf{q}_m^0[n]\ \forall m, n\}$ as follows:

$$\mathbf{q}_m^0[n] = \left(x_m^{\mathsf{init}} + d_m^{\mathsf{init}} \cos\phi_n, y_m^{\mathsf{init}} + d_m^{\mathsf{init}} \sin\phi_n \right) \ \forall m, n. \tag{38}$$

For the multi-UAV system, d_{min} denotes the minimum inter-UAV distance to ensure collision avoidance, which must be maintained as we initialize the UAVs' trajectories. Fig. 4 illustrates the initial circular trajectories for the network with three UAVs.

C. Numerical Results

1) UAV-GU Association: We first compare the performance achieved by the RSS-based method and optimized solution from (15) for UAV-GU association with 2 UAVs, 40 subchannels, initial circular UAV trajectories, $T = 20$ s, and the minimum required transmission data $D_k^{\mathsf{min}} = 5$ MB for

TABLE IV
COMPARISON OF RSS METHOD AND OPTIMIZED SOLUTION FOR UAV-GU ASSOCIATION

Max-min rate comparison (Mbps)	**Number of GUs**				
	8	**10**	**12**	**14**	**16**
RSS method	10.5821	9.1238	7.6425	6.2541	5.1228
Optimized solution using Algorithm 1	11.1149	9.8503	8.5216	7.4138	6.4206

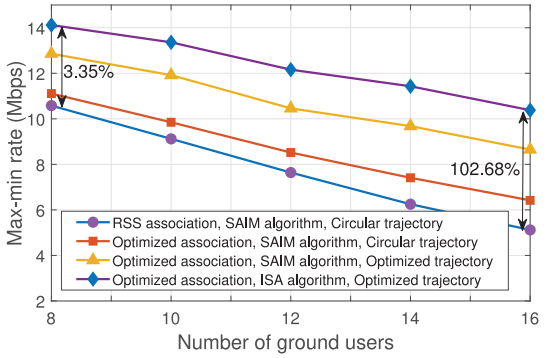

Fig. 5. Performance comparison of different schemes with 2 UAVs and $T = 20$ s.

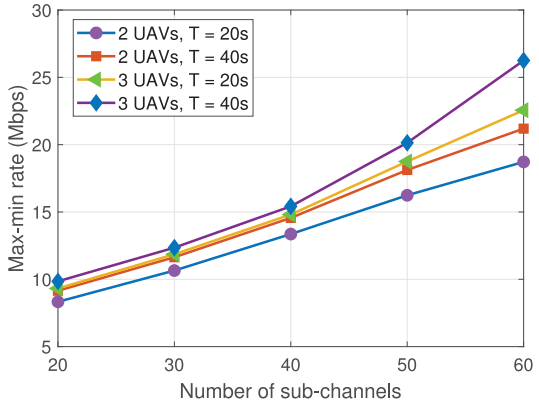

Fig. 6. Max-min rate under different number of subchannels.

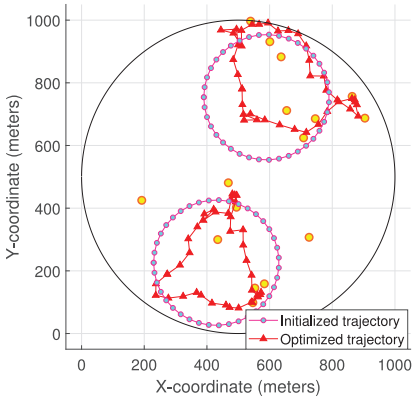

Fig. 7. Optimized trajectories for 2 UAVs, 16 GUs, and $T = 20$ s.

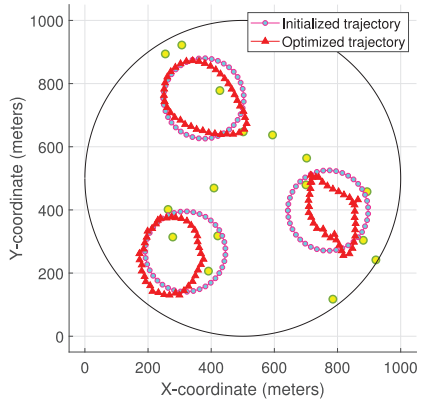

Fig. 8. Optimized trajectories for 3 UAVs, 16 GUs, and $T = 20$ s.

each GU. The max-min average rates achieved by the RSS-based method and optimized solution by using Algorithm 1 are presented in Table IV for the UAV flight period $T = 20$ s. In addition, the SAIM algorithm for subchannel assignment and the UAVs' circular trajectories are used to evaluate the system performance for different numbers of GUs. It can be seen that the optimized algorithm outperforms the RSS-based method for the UAV-GU association.

2) Subchannel Assignment: We now evaluate the performance of the proposed ISA algorithm described in Algorithm 2 and the SAIM algorithm illustrated in Fig. 3. Specifically, the max-min average rates due to different schemes are shown in Fig. 5 for the network with 2 UAVs, 40 subchannels, UAV's flight period $T = 20$ s, and the maximum velocity of UAVs $V_{\max} = 40$ (m/s). We see that the proposed design with the ISA algorithm, optimized UAV-GU association, and trajectory control achieves the highest max-min average rate among the considered schemes. In addition, the rate gaps between the proposed ISA algorithm and other schemes increase when the number of GUs increases. For a given number of subchannels, more subchannels are likely to be reused by different UAVs to meet the GUs' data transmission demands when the number of GUs increases and this will likely lead to stronger co-channel interference. The results in Fig. 5 imply that the proposed ISA algorithm can effectively manage interference and resources.

Fig. 6 illustrates the max-min average rates achieved by the proposed algorithm with different number of subchannels, for the 2-UAV and 3-UAV scenarios, 10 GUs, flight period $T = [20, 40]$ s, and the maximum velocity of UAVs $V_{\max} = 40$ (m/s). We see that the max-min average rate increases almost linearly as the number of subchannels increases in the scenario with 2 UAVs and the UAV's flight period $T = 20$ s. Furthermore, the max-min average rate for the scenario with 3 UAVs is higher than that with 2 UAVs where the rate difference becomes larger when the number of subchannels increases.

3) UAV Trajectory: Figs. 7 and 8 show the UAV trajectories for the scenarios with 2 UAVs and 3 UAVs, 16 GUs, and

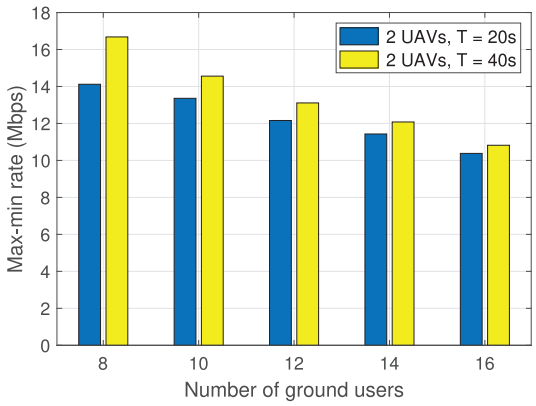

Fig. 9. Max-min rates with 2 UAVs.

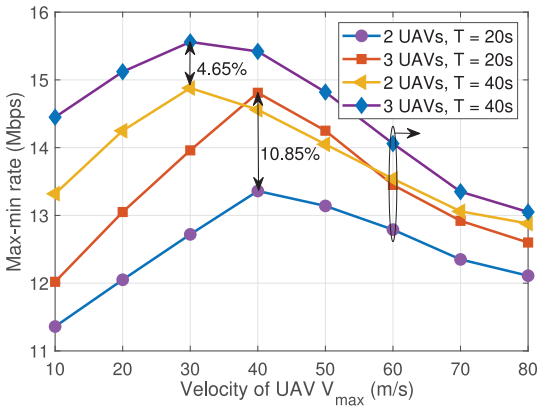

Fig. 11. Max-min rate under different velocity of UAV $V_{\max}$.

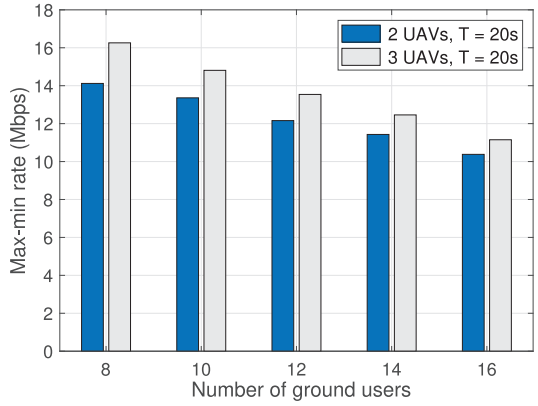

Fig. 10. Max-min rates with 2 UAVs and 3 UAVs.

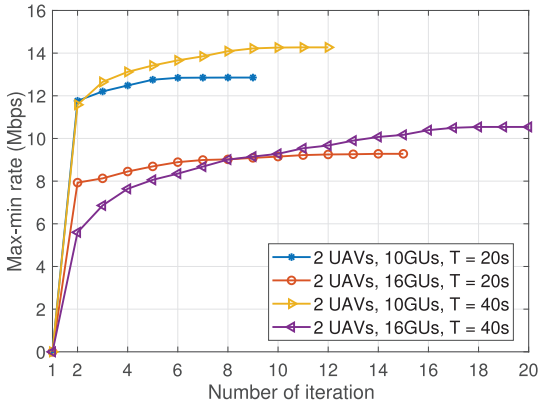

Fig. 12. Convergence of the proposed algorithm.

UAV flight period $T = 20$ s. For the setting with 2 UAVs and 16 GUs, it can be seen that the optimized trajectories are not smooth and the UAVs fly close to the corresponding clusters of GUs they are serving. Similar observations can be drawn for the scenario with 3 UAVs and 16 GUs where UAVs tend to serve the GUs closer to them.

Fig. 9 shows the max-min average rate for the 2-UAV scenario under different number of GUs and UAV flight period $T = [20, 40]$ s, maximum velocity of UAVs $V_{\max} = 40$ (m/s), and 40 subchannels. The results show that the max-min average rate increases when the UAV's flight period becomes longer. In addition, the rate difference between scenarios with the flight period $T = 20$ s and $T = 40$ s decreases when the number of GUs increases. This is because a larger number of GUs improves the radio utilization efficiency.

We show the max-min average rates achieved for scenarios with 2 UAVs and 3 UAVs under different number of GUs in Fig. 10 with parameters $T = 20$s, $V_{\max} = 40$ (m/s), and 40 subchannels. This figure shows that the max-min average rate achieved by 3 UAVs is larger than that with 2 UAVs. This is because the UAV-GU distance is typically smaller when a larger number of UAVs serves a particular number of GUs. However, the rate gap between the two scenarios decrease when the number of GUs increases due to stronger interference with the larger number of UAVs.

We study the impact of the maximum UAV's velocity $V_{\max}$ on the max-min average rate in Fig. 11 for scenarios with 2 UAVs and 3 UAVs, 10 GUs, and 40 subchannels where $V_{\max}$ varies in the range of 10–80 (m/s). It can be seen that the peaks of the max-min average rate are achieved at the maximum UAV's velocity of 40 and 30 (m/s) for $T = [20, 40]$ s, respectively. Moreover, the rate gains at the peak rates for the 3-UAV setting versus the 2-UAV setting are 4.65% and 10.85% for $V_{\max} = [30, 40]$ (m/s) and $T = [20, 40]$ s, respectively. However, this rate gain tends to decrease with the higher maximum velocity of UAVs. In fact, with the restricted network area of radius, d_m^{init}, $(\forall m)$ given in (38), the velocity of UAVs strongly impacts the initial and the optimized trajectories of UAVs. This is because when the UAVs fly faster, the inter-UAV distances can become smaller in larger portions of the flight and the co-channel interference would be stronger, especially with a large number of UAVs. Specifically, the max-min average rate with $V_{\max} \geq 60$ (m/s) in the 3-UAV deployment and $T = 20$ s is smaller than that in the 2-UAV scenario with $T = 40$ s.

The convergence of Algorithm 4 is illustrated in Fig. 12 for the network setting with 2 UAVs, 10 and 16 GUs, $T = [20, 40]$ s, $V_{\max} = 40$ (m/s) and 40 subchannels. In particular, we optimize UAV-GU association, subchannel assignment, and UAV trajectory control until convergence in each iteration of the proposed algorithm. It can be seen that the value of the objective function improves over iterations. Our algorithm converges more slowly to the feasible solution with the larger flight period T. This is because the optimization space becomes larger with a larger flight period T. Moreover,

the number of iterations increases when the number of GUs increases due to increasing complexity for algorithm.

VI. Conclusion

In this article, we studied the joint UAV-GU association, subchannel assignment, and UAV trajectory control problem to achieve fair resource sharing among GUs considering their data transmission demands and spectrum reuse. To solve the underlying MINLP problem, we use the alternating optimization approach and developed an efficient integrated algorithm. In particular, the ISA algorithm was proposed to solve the subchannel assignment subproblem.

We used SCA to solve the UAV trajectory control subproblem. Numerical results have demonstrated the effectiveness of the proposed algorithm. Specifically, the optimized UAV trajectory can result in a non-negligible rate gain compared to the case where UAVs' trajectories are set to be circular around the corresponding clusters of GUs. Moreover, we showed that the number of deployed UAVs, number of subchannels, and UAV's maximum velocity have strong impacts on the achieved max-min average rate.

Appendix A
Proof of Proposition 1

In this Appendix, we prove that the considered optimization problem is NP-hard [39]. We construct an instance of problem **(P2.1)** where subchannels assigned to GUs in different time slots. Let $\mathcal{K}, \mathcal{C}$, and $\mathcal{N}$ be three disjoint sets of GUs, subchannels, and time slots, respectively. Sets $\mathcal{K}, \mathcal{C}$, and $\mathcal{N}$ satisfy $\mathcal{K} \cap \mathcal{C} = \varnothing$, $\mathcal{K} \cap \mathcal{N} = \varnothing$, and $\mathcal{C} \cap \mathcal{N} = \varnothing$. Let $\mathcal{Q}$ be a collection of ordered triples $\mathcal{Q} \subseteq \mathcal{K} \times \mathcal{C} \times \mathcal{N}$, where each element in $\mathcal{Q}$ corresponds to a subchannel with the corresponding GU in a particular time slot, i.e., $\mathcal{Q}_i = (\mathcal{K}_i, \mathcal{C}_i, \mathcal{N}_i) \in \mathcal{Q}$. For convenience, we set $L = \min\{|\mathcal{K}|, |\mathcal{C}|, |\mathcal{N}|\}$. There exists $\mathcal{Q}' \subseteq \mathcal{Q}$ that the following holds: 1) $|\mathcal{Q}'| = |L| = \mathrm{L}$ and 2) for any two distinct triples $(\mathcal{K}_i, \mathcal{C}_i, \mathcal{N}_i) \in \mathcal{Q}'$ and $(\mathcal{K}_j, \mathcal{C}_j, \mathcal{N}_j) \in \mathcal{Q}'$, we have $i \neq j$.

Hence, $\mathcal{Q}'$ is a three dimension matching (3-DM). Since the 3-DM problem has been proved to be NP-complete in [40], the constructed instance of the problem is also NP-complete. Therefore, the problem **(P2.1)** is NP-hard.

Appendix B
Detailed Description of the Development in Section IV-C

In this Appendix, we provide details of the developments presented in Section IV-C.

1) First, $R_{k,m,c}[n]$, in constraints (14a), can be rewritten as

$$\begin{aligned}
R_{k,m,c}[n] &= \omega_{k,m}[n]\theta_{k,c}[n]W \\
&\quad \log_2\left(1+\frac{pg_{k,m}[n]}{\sum_{j=1,j\neq m}^{M}\sum_{z=1,z\neq k}^{K}\omega_{z,j}[n]\theta_{z,c}[n]pg_{k,j}[n]+\sigma^2}\right) \\
&= \omega_{k,m}[n]\theta_{k,c}[n]W \\
&\quad \log_2\left(1+\frac{\frac{p\rho_0}{H^2+\|\mathbf{q}_m[n]-\mathbf{r}_k^{\mathsf{u}}\|^2}}{\sum_{j=1,j\neq m}^{M}\sum_{z=1,z\neq k}^{K}\frac{\omega_{z,j}[n]\theta_{z,c}[n]p\rho_0}{H^2+\|\mathbf{q}_j[n]-\mathbf{r}_k^{\mathsf{u}}\|^2}+\sigma^2}\right) \\
&= \omega_{k,m}[n]\theta_{k,c}[n]W \\
&\quad \log_2\left(\frac{\sum_{j=1}^{M}\sum_{z=1}^{K}\frac{\omega_{z,j}[n]\theta_{z,c}[n]p\rho_0}{H^2+\|\mathbf{q}_j[n]-\mathbf{r}_k^{\mathsf{u}}\|^2}+\sigma^2}{\sum_{j=1,j\neq m}^{M}\sum_{z=1,z\neq k}^{K}\frac{\omega_{z,j}[n]\theta_{z,c}[n]p\rho_0}{H^2+\|\mathbf{q}_j[n]-\mathbf{r}_k^{\mathsf{u}}\|^2}+\sigma^2}\right) \\
&= \omega_{k,m}[n]\theta_{k,c}[n]W \\
&\quad \left[\log_2\left(\sum_{j=1}^{M}\sum_{z=1}^{K}\frac{\omega_{z,j}[n]\theta_{z,c}[n]p\rho_0}{H^2+\left\|\mathbf{q}_j[n]-\mathbf{r}_k^{\mathsf{u}}\right\|^2}+\sigma^2\right)\right. \\
&\quad \left.-\log_2\left(\sum_{j=1,j\neq m}^{M}\sum_{z=1,z\neq k}^{K}\frac{\omega_{z,j}[n]\theta_{z,c}[n]p\rho_0}{H^2+\left\|\mathbf{q}_j[n]-\mathbf{r}_k^{\mathsf{u}}\right\|^2}+\sigma^2\right)\right] \\
&= \omega_{k,m}[n]\theta_{k,c}[n]W\Big(\hat{R}_{k,m,c}[n]-\tilde{R}_{k,m,c}[n]\Big). \qquad (39)
\end{aligned}$$

2) Second, the upper bound of $\tilde{R}_{k,m,c}[n]$ can be expressed as

$$\begin{aligned}
\tilde{R}^{\mathsf{ub}}_{k,m,c}[n] &= \log_2\left(\sum_{j=1,j\neq m}^{M}\sum_{z=1,z\neq k}^{K}R^{\mathsf{Ab},r}_{z,j,c,k,m}[n]+\sigma^2\right) \\
&\quad + \sum_{j=1,j\neq m}^{M}\sum_{z=1,z\neq k}^{K}\frac{\log_2(e)}{\sum_{j=1,j\neq m}^{M}\sum_{z=1,z\neq k}^{K}R^{\mathsf{Ab},r}_{z,j,c,k,m}[n]+\sigma^2} \\
&\quad \Big(R^{\mathsf{Ab}}_{z,j,c,k,m}[n]-R^{\mathsf{Ab},r}_{z,j,c,k,m}[n]\Big). \qquad (40)
\end{aligned}$$

3) Third, based on the first-order Taylor expansion at the given points $R^{\mathsf{Ab},r}_{z,j,c,k,m}[n]$ and $S^r_{k,j}[n]$ in the rth iteration of the approximation process, it can be approximated as

$$\begin{aligned}
&R^{\mathsf{Ab}}_{z,j,c,k,m}[n]S_{k,j}[n] \\
&\le \frac{1}{4}\Bigg[\Big(R^{\mathsf{Ab}}_{z,j,c,k,m}[n]+S_{k,j}[n]\Big)^2-2\Big(R^{\mathsf{Ab},r}_{z,j,c,k,m}[n]-S^r_{k,j}[n]\Big) \\
&\qquad \times\Big(R^{\mathsf{Ab}}_{z,j,c,k,m}[n]-S_{k,j}[n]\Big) \\
&\qquad +\Big(R^{\mathsf{Ab},r}_{z,j,c,k,m}[n]-S^r_{k,j}[n]\Big)^2\Bigg]\triangleq R^{\mathsf{App},r}[n]. \qquad (41)
\end{aligned}$$

Appendix C
Proof of Proposition 2

In this Appendix, we prove that Algorithm 4 creates a non-decreasing sequence of objective values of problem **(P)** and converges to a feasible solution. First, it can be verified after the initialization step or after each r-iteration of the approximation process, we achieve a feasible solution of $\mathbf{\Omega}^r$, $\mathbf{\Theta}^r$, and $\mathbf{Q}^r$. For step 2 of Algorithm 4, since the optimal solution of **(P1.1)** is obtained for given $\mathbf{\Theta}^r$ and $\mathbf{Q}^r$, we have

$$\eta\big(\mathbf{\Omega}^r, \mathbf{\Theta}^r, \mathbf{Q}^r\big) \le \eta\Big(\mathbf{\Omega}^{r+1}, \mathbf{\Theta}^r, \mathbf{Q}^r\Big) \qquad (42)$$

where $\eta(\mathbf{\Omega}, \mathbf{\Theta}, \mathbf{Q})$ is defined in the formulation for problem (14). Moreover, for given $\mathbf{\Omega}^{r+1}$, $\mathbf{\Theta}^r$, and $\mathbf{Q}^r$ obtained in step 3 of Algorithm 4, it follows that:

$$\eta\Big(\mathbf{\Omega}^{r+1}, \mathbf{\Theta}^r, \mathbf{Q}^r\Big) \le \eta\Big(\mathbf{\Omega}^{r+1}, \mathbf{\Theta}^{r+1}, \mathbf{Q}^r\Big). \qquad (43)$$

This is because problem **(P2.1)** is solved under the ISA algorithm presented in Section IV-B. Finally, for given $\mathbf{\Omega}^{r+1}$, $\mathbf{\Theta}^{r+1}$, and $\mathbf{Q}^r$ obtained in step 4 of Algorithm 4, we have

$$\eta\Big(\mathbf{\Omega}^{r+1}, \mathbf{\Theta}^{r+1}, \mathbf{Q}^r\Big) \overset{(a)}{\le} \eta^{\mathsf{lb,r}}_{\mathsf{trj}}\Big(\mathbf{\Omega}^{r+1}, \mathbf{\Theta}^{r+1}, \mathbf{Q}^{r+1}\Big)$$

$$\overset{(b)}{\leq} \eta\left(\boldsymbol{\Omega}^{r+1}, \boldsymbol{\Theta}^{r+1}, \mathbf{Q}^{r+1}\right) \tag{44}$$

where we define $\eta_{\text{trj}}^{\text{lb,r}}(\boldsymbol{\Omega}, \boldsymbol{\Theta}, \mathbf{Q}) = \eta_{\text{trj}}^{r}$ as the objective value of problem (35). And (a) holds since Algorithm 4 achieves the solution $\mathbf{Q}^{r+1}$ for given $\boldsymbol{\Omega}^{r+1}$ and $\boldsymbol{\Theta}^{r+1}$; (b) holds since the objective value of problem (35) is the lower bound of the objective of its original problem (23) at $\mathbf{Q}^{r+1}$ because the SCA method is applied. Using the results in (42)–(44), we obtain

$$\eta(\boldsymbol{\Omega}, \boldsymbol{\Theta}, \mathbf{Q}) \leq \eta\left(\boldsymbol{\Omega}^{r+1}, \boldsymbol{\Theta}^{r+1}, \mathbf{Q}^{r+1}\right) \tag{45}$$

which indicates that the objective value of problem **(P)** is nondecreasing after each iteration of Algorithm 4. Since the objective value of problem **(P)** is upper bounded by a finite value, Algorithm 4 is guaranteed to converge to a feasible solution. This completes the proof.

REFERENCES

[1] V. W. Wong, R. Schober, D. W. K. Ng, and L.-C. Wang, *Key Technologies for 5G Wireless Systems*. Cambridge, U.K.: Cambridge Univ. Press, 2017.

[2] *IEEE 5G and Beyond Technology Roadmap White Paper*, IEEE Future Networks, New York, NY, USA, Oct. 2017. [Online]. Available: https://futurenetworks.ieee.org/images/files/pdf/ieee-5g-roadmap-white-paper.pdf

[3] B. Li, Z. Fei, and Y. Zhang, "UAV communications for 5G and beyond: Recent advances and future trends," *IEEE Internet Things J.*, vol. 6, no. 2, pp. 2241–2263, Apr. 2019.

[4] M. Marchese, A. Moheddine, and F. Patrone, "IoT and UAV integration in 5G hybrid terrestrial-satellite networks," *Sensors*, vol. 19, no. 17, p. 3704, Aug. 2019.

[5] M. Mozaffari, W. Saad, M. Bennis, Y.-H. Nam, and M. Debbah, "A tutorial on UAVs for wireless networks: Applications, challenges, and open problems," *IEEE Commun. Surveys Tuts.*, vol. 21, no. 3, pp. 2334–2360, 3rd Quart., 2019.

[6] Y. Zeng, J. Lyu, and R. Zhang, "Cellular-connected UAV: Potential, challenges and promising technologies," *IEEE Wireless Commun.*, vol. 26, no. 1, pp. 120–127, Feb. 2019.

[7] S. Zhang, Y. Zeng, and R. Zhang, "Cellular-enabled UAV communication: A connectivity-constrained trajectory optimization perspective," *IEEE Trans. Commun.*, vol. 67, no. 3, pp. 2580–2604, Mar. 2019.

[8] C. Zhan, Y. Zeng, and R. Zhang, "Energy-efficient data collection in UAV enabled wireless sensor network," *IEEE Wireless Commun. Lett.*, vol. 7, no. 3, pp. 328–331, Jun. 2018.

[9] M. B. Ghorbel, D. Rodríguez-Duarte, H. Ghazzai, M. J. Hossain, and H. Menouar, "Joint position and travel path optimization for energy efficient wireless data gathering using unmanned aerial vehicles," *IEEE Trans. Veh. Technol.*, vol. 68, no. 3, pp. 2165–2175, Mar. 2019.

[10] V. Sharma, R. Kumar, and R. Kaur, "UAV-assisted content-based sensor search in IoTs," *Electron. Lett.*, vol. 53, no. 11, pp. 724–726, May 2017.

[11] Y. Zeng, R. Zhang, and T. J. Lim, "Throughput maximization for UAV-enabled mobile relaying systems," *IEEE Trans. Commun.*, vol. 64, no. 12, pp. 4983–4996, Dec. 2016.

[12] J. Fan, M. Cui, G. Zhang, and Y. Chen, "Throughput improvement for multi-hop UAV relaying," *IEEE Access*, vol. 7, pp. 147732–147742, Dec. 2019.

[13] W. Wang *et al.*, "Energy-constrained UAV-assisted secure communications with position optimization and cooperative jamming," *IEEE Trans. Commun.*, vol. 68, no. 7, pp. 4476–4489, Jul. 2020.

[14] H. Wang, J. Wang, G. Ding, J. Chen, Y. Li, and Z. Han, "Spectrum sharing planning for full-duplex UAV relaying systems with underlaid D2D communications," *IEEE J. Sel. Areas Commun.*, vol. 36, no. 9, pp. 1986–1999, Sep. 2018.

[15] R. Fan, J. Cui, S. Jin, K. Yang, and J. An, "Optimal node placement and resource allocation for UAV relaying network," *IEEE Commun. Lett.*, vol. 22, no. 4, pp. 808–811, Apr. 2018.

[16] A. Al-Hourani, S. Kandeepan, and S. Lardner, "Optimal LAP altitude for maximum coverage," *IEEE Wireless Commun. Lett.*, vol. 3, no. 6, pp. 569–572, Dec. 2014.

[17] J. Lyu, Y. Zeng, R. Zhang, and T. J. Lim, "Placement optimization of UAV-mounted mobile base stations," *IEEE Commun. Lett.*, vol. 21, no. 3, pp. 604–607, Mar. 2017.

[18] P. Li and J. Xu, "Placement optimization for UAV-enabled wireless networks with multi-hop backhaul," *J. Commun. Inf. Netw.*, vol. 3, no. 4, pp. 64–73, Dec. 2018.

[19] M. D. Nguyen, T. M. Ho, L. B. Le, and A. Girard, "UAV placement and bandwidth allocation for UAV based wireless networks," in *Proc. IEEE Global Commun. Conf. (GLOBECOM)*, Dec. 2019, pp. 1–6.

[20] H. Tang, Q. Wu, and B. Li, "An efficient solution for joint power and trajectory optimization in UAV-enabled wireless network," *IEEE Access*, vol. 7, pp. 59640–59652, May 2019.

[21] M. T. Nguyen and L. B. Le, "Flight scheduling and trajectory control in UAV-based wireless networks," in *Proc. IEEE Wireless Commun. Netw. Conf. (WCNC)*, May 2020, pp. 1–6.

[22] Q. Wu, Y. Zeng, and R. Zhang, "Joint trajectory and communication design for multi-UAV enabled wireless networks," *IEEE Trans. Wireless Commun.*, vol. 17, no. 3, pp. 2109–2121, Mar. 2018.

[23] H. Mei, K. Yang, Q. Liu, and K. Wang, "Joint trajectory-resource optimization in UAV-enabled edge-cloud system with virtualized mobile clone," *IEEE Internet Things J.*, vol. 7, no. 7, pp. 5906–5921, Jul. 2020.

[24] F. Zeng *et al.*, "Resource allocation and trajectory optimization for QoE provisioning in energy-efficient UAV-enabled wireless networks," *IEEE Trans. Veh. Technol.*, vol. 69, no. 7, pp. 7634–7647, Jul. 2020.

[25] Y. Huang, M. Cui, G. Zhang, and W. Chen, "Bandwidth, power and trajectory optimization for UAV base station networks with backhaul and user QoS constraints," *IEEE Access*, vol. 8, pp. 67625–67634, Apr. 2020.

[26] S. Zhang, H. Zhang, B. Di, and L. Song, "Cellular UAV-to-X communications: Design and optimization for multi-UAV networks," *IEEE Trans. Wireless Commun.*, vol. 18, no. 2, pp. 1346–1359, Feb. 2019.

[27] Y. Cai, Z. Wei, R. Li, D. W. K. Ng, and J. Yuan, "Joint trajectory and resource allocation design for energy-efficient secure UAV communication systems," *IEEE Trans. Commun.*, vol. 68, no. 7, pp. 4536–4553, Jul. 2020.

[28] Q. Wu and R. Zhang, "Common throughput maximization in UAV-enabled OFDMA systems with delay consideration," *IEEE Trans. Commun.*, vol. 66, no. 12, pp. 6614–6627, Dec. 2018.

[29] M. D. Nguyen, T. M. Ho, L. B. Le, and A. Girard, "UAV trajectory and sub-channel assignment for UAV based wireless networks," in *Proc. IEEE Wireless Commun. Netw. Conf. (WCNC)*, May 2020, pp. 1–6.

[30] M. D. Nguyen, L. B. Le, and A. Girard, "Trajectory control and resource allocation for UAV-based networks with wireless backhauls," in *Proc. IEEE Int. Conf. Commun. (ICC)*, Jun. 2021, pp. 1–6.

[31] P. Yu *et al.*, "Capacity enhancement for 5G networks using MmWave aerial base stations: Self-organizing architecture and approach," *IEEE Wireless Commun.*, vol. 25, no. 4, pp. 58–64, Aug. 2018.

[32] A. Trotta, M. D. Felice, F. Montori, K. R. Chowdhury, and L. Bononi, "Joint coverage, connectivity, and charging strategies for distributed UAV networks," *IEEE Trans. Robot.*, vol. 34, no. 4, pp. 883–900, Aug. 2018.

[33] M. Grant and S. Boyd, "CVX: MATLAB software for disciplined convex programming, version 2.1," Dec. 2018. [Online]. Available: http://cvxr.com/cvx/

[34] H. H. Kha, H. D. Tuan, and H. H. Nguyen, "Fast global optimal power allocation in wireless networks by local D.C. programming," *IEEE Trans. Wireless Commun.*, vol. 11, no. 2, pp. 510–515, Feb. 2012.

[35] T. D. Hoang, L. B. Le, and T. Le-Ngoc, "Energy-efficient resource allocation for D2D communications in cellular networks," *IEEE Trans. Veh. Technol.*, vol. 65, no. 9, pp. 6972–6986, Sep. 2016.

[36] Z. Li, M. Chen, C. Pan, N. Huang, Z. Yang, and A. Nallanathan, "Joint trajectory and communication design for secure UAV networks," *IEEE Commun. Lett.*, vol. 23, no. 4, pp. 636–639, Apr. 2019.

[37] *Online Video Test Media*. [Online]. Available: https://media.xiph.org/video/derf/ (Accessed: May 10, 2021).

[38] T. Kanungo, D. M. Mount, N. S. Netanyahu, C. D. Piatko, R. Silverman, and A. Y. Wu, "An efficient k-means clustering algorithm: Analysis and implementation," *IEEE Trans. Pattern Anal. Mach. Intell.*, vol. 24, no. 7, pp. 881–892, Jul. 2002.

[39] W. J. Cook, W. H. Cunningham, W. R. Pulleyblank, and A. Schrijver, *Combinatorial Optimization*. New York, NY, USA: Wiley, 1997.

[40] M. R. Garey and D. S. Johnson, "Computers and intractability: A guide to the theory of NP-completeness," 1st ed. New York, NY, USA: Freeman, 1979, pp. 50–53.

Minh Dat Nguyen (Graduate Student Member, IEEE) received the B.Eng. degree in electronics and communications engineering from the Posts and Telecommunications Institute of Technology, Hanoi, Vietnam, in 2016, and the M.Eng. degree in communications network from Japan Advanced Institute of Science and Technology, Nomi, Japan, in 2018. He is currently pursuing the Ph.D. degree with the Institut National de la Recherche Scientifique–Énergie, Matériaux et Télécommunications, Université du Québec, Montréal, QC, Canada.

His current research interests include UAV communications, radio resource management, 5G new radio, and AI for wireless communications.

Long Bao Le (Senior Member, IEEE) received the B.Eng. degree in electrical engineering from Ho Chi Minh City University of Technology, Ho Chi Minh City, Vietnam, in 1999, the M.Eng. degree in telecommunications from the Asian Institute of Technology, Khlong Nueng, Thailand, in 2002, and the Ph.D. degree in electrical engineering from the University of Manitoba, Winnipeg, MB, Canada, in 2007.

He was a Postdoctoral Researcher with the Massachusetts Institute of Technology, Cambridge, MA, USA, from 2008 to 2010, and University of Waterloo, Waterloo, ON, Canada, from 2007 to 2008. Since 2010, he has been with the Institut National de la Recherche Scientifique, Université du Québec, Montréal, QC, Canada, where he is currently a Full Professor. He has coauthored the books *Radio Resource Management in Multi-Tier Cellular Wireless Networks* (Wiley, 2013) and *Radio Resource Management in Wireless Networks: An Engineering Approach* (Cambridge University Press, 2017). His research interests include smartgrids, intelligent transportation systems, and emerging enabling technologies for 5G and beyond wireless systems.

Dr. Le was a member of the editorial boards of IEEE TRANSACTIONS ON WIRELESS COMMUNICATIONS and IEEE COMMUNICATIONS SURVEYS AND TUTORIALS.

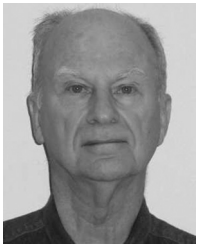

André Girard (Member, IEEE) received the Ph.D. degree in physics from the University of Pennsylvania, Philadelphia, PA, USA, in 1971.

He was an Adjunct Professor with INRS-EMT and the École Polytechnique of Montréal, Montreal, QC, Canada. He was a Faculty Member of INRS-Telecommunications until 2004. During that time, he involved in various aspects of telecommunication networks, and in particular with performance evaluation, routing, dimensioning, and reliability. He has made numerous theoretical and algorithmic contributions to the design of telephone, ATM, IP, and wireless networks.